Hydrogen bond dynamics in bulk alcohols

Shinokita, Keisuke; Cunha, Ana V.; Jansen, Thomas L. C.; Pshenichnikov, Maxim S.

Published in:
Journal of Chemical Physics

DOI:
10.1063/1.4921574

Publication date:
2015

Hydrogen bond dynamics in bulk alcohols

Keisuke Shinokita, Ana V. Cunha, Thomas L. C. Jansen, and Maxim S. Pshenichnikov

Citation: The Journal of Chemical Physics **142**, 212450 (2015); doi: 10.1063/1.4921574
View online: https://doi.org/10.1063/1.4921574
View Table of Contents: http://aip.scitation.org/toc/jcp/142/21
Published by the American Institute of Physics

Hydrogen bond dynamics in bulk alcohols

Keisuke Shinokita, Ana V. Cunha, Thomas L. C. Jansen, and Maxim S. Pshenichnikov[a)]
Zernike Institute for Advanced Materials, University of Groningen, Nijenborgh 4, 9747 AG Groningen, The Netherlands

(Received 4 February 2015; accepted 12 May 2015; published online 28 May 2015)

Hydrogen-bonded liquids play a significant role in numerous chemical and biological phenomena. In the past decade, impressive developments in multidimensional vibrational spectroscopy and combined molecular dynamics–quantum mechanical simulation have established many intriguing features of hydrogen bond dynamics in one of the fundamental solvents in nature, water. The next class of a hydrogen-bonded liquid—alcohols—has attracted much less attention. This is surprising given such important differences between water and alcohols as the imbalance between the number of hydrogen bonds, each molecule can accept (two) and donate (one) and the very presence of the hydrophobic group in alcohols. Here, we use polarization-resolved pump-probe and 2D infrared spectroscopy supported by extensive theoretical modeling to investigate hydrogen bond dynamics in methanol, ethanol, and isopropanol employing the OH stretching mode as a reporter. The sub-ps dynamics in alcohols are similar to those in water as they are determined by similar librational and hydrogen-bond stretch motions. However, lower density of hydrogen bond acceptors and donors in alcohols leads to the appearance of slow diffusion-controlled hydrogen bond exchange dynamics, which are essentially absent in water. We anticipate that the findings herein would have a potential impact on fundamental chemistry and biology as many processes in nature involve the interplay of hydrophobic and hydrophilic groups. © *2015 AIP Publishing LLC.* [http://dx.doi.org/10.1063/1.4921574]

I. INTRODUCTION

Hydrogen bond (HB) dynamics in liquids plays a significant role in chemical and biological reactions. In the past decade, impressive advances in 2D infrared (IR) spectroscopy[1–3] and combined molecular dynamics (MD)–quantum-classical spectral calculations have placed HB dynamics of liquid water in the research spotlight due to their fundamental role in nature.[4–6] Most of the investigation of aqueous HB dynamics was accomplished by using the OH/OD stretching mode as a reporter due to the OH frequency sensitivity to the surrounding HB network. The HB exchange event was identified as occurring along a bifurcation coordinate,[7] which necessitates a large reorientational jump of the involved HB donor.[4] Furthermore, the importance of interactions between the hydrogen bonded solvent and biological molecules has been highlighted.[8–12]

Alcohols present another example of hydrogen-bonded liquids that differ from water in a number of important aspects. First, in alcohols, the number of possible donated HBs per molecule (one) is half the number of possible accepted HBs (two). This disrupts the three dimensional HB network so characteristic for water and results in a reduced dimensionality of alcohol HB networks. Next, alcohol molecules are by definition amphiphilic, i.e., contain both nonpolar alkyl hydrophobic and polar hydroxyl hydrophilic parts. This adds another complexity to the HB dynamics in alcohols nonexistent in water because some hydroxyl groups experience hydrophobic solvation.[13–15] The size and shape of alcohol molecules can be easily varied, e.g., by changing the alkyl chain length or by going from primary to secondary or tertiary alcohols, which emphasizes the effect of the hydrophobic parts in the HB network. Finally, alcohols unlike water are miscible with a wide variety of both polar and nonpolar solvents.

Many of the aforementioned properties have been explored by ultrafast spectroscopy to elucidate the HB dynamics in alcohols mainly dissolved in CCl_4, with the main focus on the vibrational energy relaxation (VER). It was demonstrated that the excitation of OH stretching mode in HB clusters is followed by VER in the sub-ps or ps time range with the subsequent HB dissociation.[16–19] As the OH absorption band is strongly heterogeneous, frequency-dependent vibrational lifetimes were observed.[20] The vibrational lifetime in clusters is faster than in monomer alcohols dissolved in CCl_4, where the VER dynamics are in the order of tens of ps.[21–23] These results suggest that HB breaking is a final acceptor mode in VER, and the HB strength alters the VER channels.[24,25] It was proposed that direct HB breaking in the excited molecules occurs in 200 fs via intramolecular energy transfer, while indirect HB breaking in different molecules via intermolecular energy transfer takes ~2 ps.[18] The HB reformation was reported to occur on ~10 ps time scales and even a component slower than 10 ns was reported. The reorientation was reported to happen on the time scales of 1.7 ps and 17 ps in the isotope diluted samples of methanol.[18]

It is, however, still an open question whether the properties observed in alcohol clusters including the larger fragility of the stronger HB are special to the clusters isolated in the CCl_4 solvent or are more general and also applicable to bulk alcohols, where the HB network extends over numerous molecules. Very

a)e-mail: Maxim.Pchenitchnikov@RuG.nl

recently, Mazur *et al.* studied bulk deuterated alcohols by IR polarization-sensitive spectroscopy.[26] In particular, they found extremely long reorientational times (exceeding 15 ps) and frequency-dependent relaxation times of the OD stretch, which were explained by the Fermi resonance to the CH_3 rocking mode.

Here, we use polarization sensitive pump-probe and 2D IR spectroscopy on the OH stretching mode to reveal HB dynamics in three alcohols: methanol, ethanol, and isopropanol. The experimental results are supported by a theoretical investigation, which combines MD simulations to elucidate the molecular picture of HB dynamics with spectral simulations to make a bridge to the experimental observables and to analyze the HB dynamics beyond the experimental time limit imposed by OH population relaxation. Relaxation times of the OH stretch are found independent of frequency and to increase with the size of the alcohol molecule. From 2D IR experiments, we conclude that the OH dynamics occur at two prime time scales: the fast, ~100 fs component is rooted to OH librations and HB stretching, and the slow, component arises from diffusive motion. The anisotropy also decays on two time scales with weakly alcohol-dependent, 200-300 fs hydroxyl wobbling-in-a-cone type of motion, and strongly alcohol-dependent, 5-20 ps orientational-jump HB exchange. We conclude that different types of molecular motion manifest themselves differently in the spectroscopic techniques: the frequency fluctuations experienced by the OH *acceptors* are most visible in 2D IR, while reorientation of the *donors* governs the anisotropy transients.

II. EXPERIMENTAL

For 2D measurements, we used a pump-probe geometry with two collinear pump pulses (~3 μJ/pulse) and one probe pulse, all centered at 3350 cm^{-1} with ~75 fs in duration.[27] The infrared pulses were generated by optical parametric amplification (OPA) following a home-built amplified Ti:sapphire laser (repetition rate 1 kHz, central wavelength 800 nm, pulse duration ~30 fs, energy 600 μJ/pulse).

At the given waiting time between the probe and one of the pump pulses, the other pump pulse was scanned from −400 to 400 fs creating the coherence time interval. The spectrum of the probe pulse was measured using a 64 element MCT coupled spectrometer providing the ω_3-dimension. To remove the contribution from an unwanted pulse sequence in early waiting time (until the 400 fs), the signal with the positive coherence time (i.e., in which the probe pulse followed the two pump pulses) was mirrored to the negative coherence time. The real part of the Fourier transformation over the coherence time provided the ω_1-dimension thereby producing the purely absorptive 2D spectra. The polarization between two pump pulses and the probe pulse is set as magic angle ~54.7° to produce isotropic 2D spectra.

Frequency-resolved pump-probe signals were measured using a single pump pulse. For anisotropy measurement, the parallel and perpendicular polarizations of the signal were measured separately by the spectrometer, and anisotropy was calculated using the following equation:

$$R = \frac{\Delta OD_{||} - \Delta OD_{\perp}}{\Delta OD_{||} + 2\Delta OD_{\perp}}, \quad (1)$$

where ΔOD is the change in optical density with the pump pulse on/off.

To avoid effects of intermolecular coupling of the OH oscillators,[28–31] the samples of methanol (CH_3OH), ethanol (C_2H_5OH), and isopropanol (C_3H_7OH) were diluted in the respective alcohols with deuterated hydroxyl group. For simplicity, in the rest of the paper, we will refer to the samples in the deuterated bath simply as alcohols. All chemicals were obtained from Sigma-Aldrich and used without further purification. Solutions of ~6% native alcohols were placed in a 50 μm-thick free-standing sapphire jet which resulted in OD ~ 0.6 at the maximum of OH-stretch absorption. The circulatory pump system was purged with nitrogen to minimize water absorption from the air. All experiments were performed at room temperature (295 K).

III. MODELING

MD simulations were performed in GROMACS[32] using the Optimized Potentials for Liquid Simulations-all atoms (OPLS/AA) force field[33] for the alcohols using 301, 200, and 216 molecules for methanol, ethanol, and isopropanol, respectively. The Lennard-Jones and Coulomb interaction were truncated at a 1.1 nm cutoff. The long-range Coulomb interactions were accounted for using the particle mesh Ewald scheme.[34] After initial equilibration, a 500 ps trajectory with snapshots stored at 10 fs intervals was obtained for each alcohol. The simulations were performed at 298.15 K using the constant equilibrium volume and a Berendsen thermostat.[35] All bonds were constrained using the LINCS algorithm.[36] Snapshots from MD illustrating the HB structures for the three different alcohols in the simulation boxes are presented in Figure 1. For methanol, long hydrogen bonded chains are clearly identifiable, whereas in isopropanol, the hydrogen bonded chains are shorter and more bended as a consequence of the steric repulsion of the hydrophobic groups. In ethanol, hydrogen bonded structures are intermediate between methanol and isopropanol.

A time-dependent vibrational Hamiltonian was generated for the spectral simulations using an electrostatic mapping for the OH stretch vibration originally developed for water[38,39] of the following form:

$$H(t) = \sum_i^N \omega_i(t) B_i^{\dagger} B_i - \Delta_i/2 B_i^{\dagger} B_i^{\dagger} B_i B_i + \vec{\mu}_i(t)\vec{E}(t)(B_i^{\dagger} + B_i). \quad (2)$$

Here, $B_i^{\dagger}$ and B_i are the usual Bosonic creation and annihilation operators, $\omega_i(t)$ is the time-dependent fundamental frequency for each OH-stretch vibration, and Δ_i stands for the anharmonicity (fixed at 200 cm^{-1}). The transition dipoles are given by $\vec{\mu}_i(t)$, and the summation runs over all OH stretches in the simulation box. The use of this form of the Hamiltonian implies that the harmonic rule is applied for the $|1\rangle \rightarrow |2\rangle$ transition dipoles.

The frequencies and transition dipoles were determined for all OH stretches for all stored snapshots along the MD trajectory using the electrostatic mapping for the OH stretch

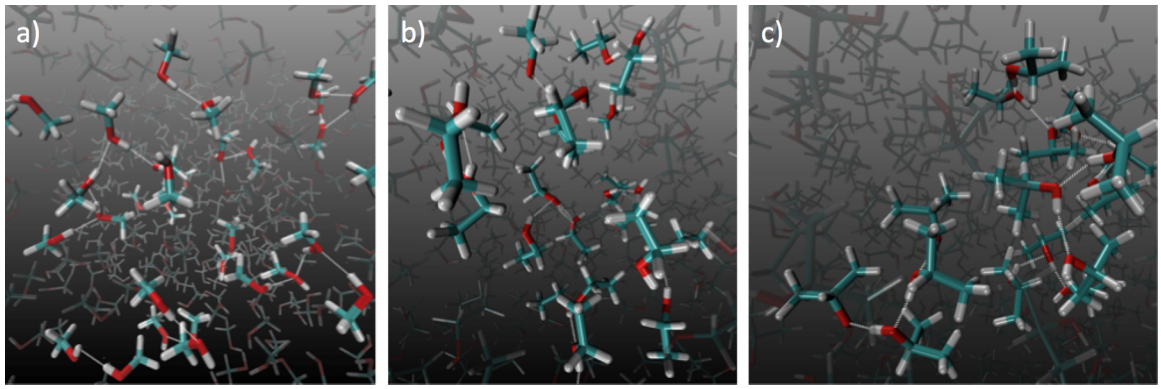

FIG. 1. Illustration of typical hydrogen bond networks in methanol ((a), multimedia view Fig1a.mov), ethanol (b), and isopropanol ((c), multimedia view Fig1c.mov) using snapshots from the MD simulations. Oxygen atoms are red and hydrogen atoms white. Hydrogen bonds are highlighted as dashed white lines. The snapshots were generated with the Visual Molecular Dynamics (VMD) software.[37] (Multimedia view) [URL: http://dx.doi.org/10.1063/1.4921574.1] [URL: http://dx.doi.org/10.1063/1.4921574.2]

vibration originally developed for water.[38,40] This approach allows calculating the averaged response over all OH-stretch vibrations by treating them independently. This implies the approximation that each OH-stretch experiences a classical environment of isotopically unlabeled solvent molecules, but the quantum mechanical coupling is omitted leading to an effective description of independent OH oscillators as in an isotope diluted experiment. However, the mass of the solvent hydrogen atoms is smaller than in the experiment, which may lead to too fast motion in the simulations. Nonetheless, this type of approximation has been successfully applied for the study of HB dynamics in water before.[38,41,42] The linear absorption and 2D IR were obtained using the NISE simulation code[43] with coherence times of 320 fs and sampling at 1 ps intervals along the 500 ps trajectories. A 130 cm^{-1} redshift of all simulated spectra was introduced to match the experimental position of absorption peaks.

IV. RESULTS

A. Linear absorption

Figure 2(a) shows the linear absorption spectra of the OH stretching mode of methanol, ethanol, and isopropanol. All experimental spectra peak at ~3350 cm^{-1} and have decreasing widths as the alcohol size increases. The fact that the peak positions essentially coincide in different alcohols suggests that the average hydrogen bond strength is not significantly affected by the size or shape of the alkyl chains. The appreciable width of the spectra was attributed to inhomogeneous broadening,[19] with larger broadening in longer alcohols. This trend in broadening is well reproduced in the simulations (Fig. 2(b)), although the calculated spectra are slightly narrower. Also, in the simulations, a blue shift of about 25 cm^{-1} is observed for methanol as compared to the other alcohols. This suggests that the employed force field,[33] where identical charges are used for the three alcohols, either slightly overestimates the hydrogen bonding in the larger alcohols or underestimates it in methanol. This may potentially result from the neglect of polarizability in the utilized force fields.

Unlike in alcohol clusters in CCl_4[45] where clearly distinctive spectral features originate from different HB configurations (Fig. 3), the bulk alcohol spectra look quite similar to that of HDO:D_2O, despite being red-shifted and narrower. The overall redshift here does not reflect the strength of HBs, but results from the larger than in water mass attached to the oxygen, as confirmed by gas-phase calculations and absorption spectra of alcohol molecules diluted in acetonitrile.[46]

The narrower width of the alcohol spectra as compared to water originates from less diverse HB structures. To highlight this point, HB analysis was performed by identifying all hydrogen bonded alcohol pairs, where the OH distance (r) was below 2.5 Å and the OHO angle (β) was below 30°.[47] If an alcohol molecule using this definition was found to donate more than one HB, only the HB with the shortest OH distance was used. For each alcohol molecule, the number of donated and accepted HBs along the trajectory was counted and the

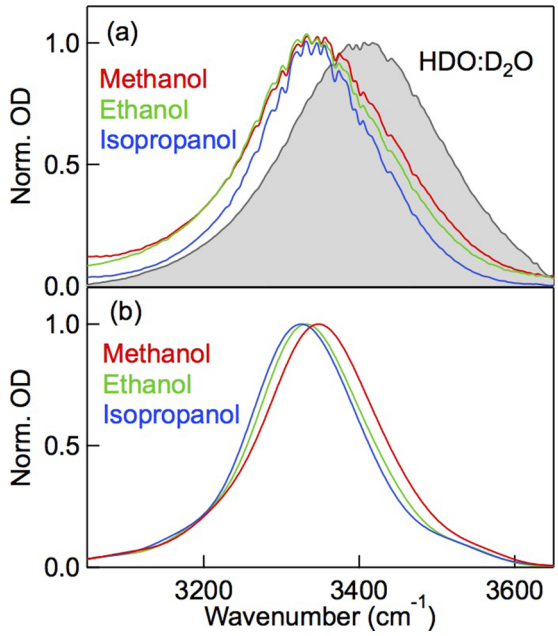

FIG. 2. Normalized experimental (a) and simulated (b) linear absorption spectra of hydroxyl stretch in CH_3OH/CH_3OD (red), C_2H_5OH/C_2H_5OD (green), and C_3H_7OH/C_3H_7OD (blue). The HDO:D_2O absorption (shaded contour) is shown for comparison.

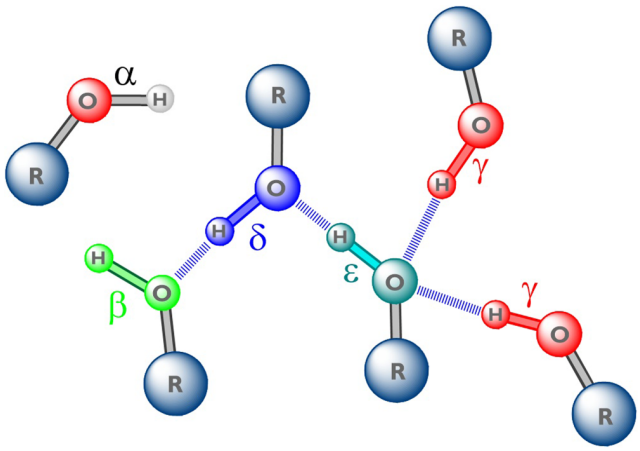

FIG. 3. Schematics of the five different HB configurations in alcohols.[44] The blue shaded lines illustrate HBs and R denotes the alkane chains. The nomenclature is the following: α-molecules have no HBs, β accepts one or two HBs, γ donates a HB, δ accepts and donates a HB, and ε accepts two and donates one HB.

alcohol molecules were categorized using the convention presented in Fig. 3.

Frequency distributions for each of the five HB categories are shown in Fig. 4. The α and β types that do not donate HBs absorb at frequencies above 3570 cm^{-1}, while the other types absorb at lower frequencies. The more hydrogen bonds the alcohol molecule accepts, the lower the OH stretch frequency it has. The δ type dominates in all three alcohols, while the α and β types are slightly more abundant in isopropanol than in the smaller alcohols. In the absorption spectra, the contribution from the latter types is, however, heavily suppressed due to pronounced non-Condon effects.[48] In the larger alcohols, the γ and ε types are slightly less abundant, which explains the narrowing of the linear absorption spectra due to the more homogeneous distribution of HB environments. The average frequencies and peak widths for the different HB types vary by about 5 cm^{-1} between the different alcohols. This is minimal as compared to the frequency differences observed between different HB configurations. We can also understand why the spectral width in all alcohols is narrower than in water: in water, many HB environments coexist,[30,42,49–51] while the δ-type is dominant in alcohols.

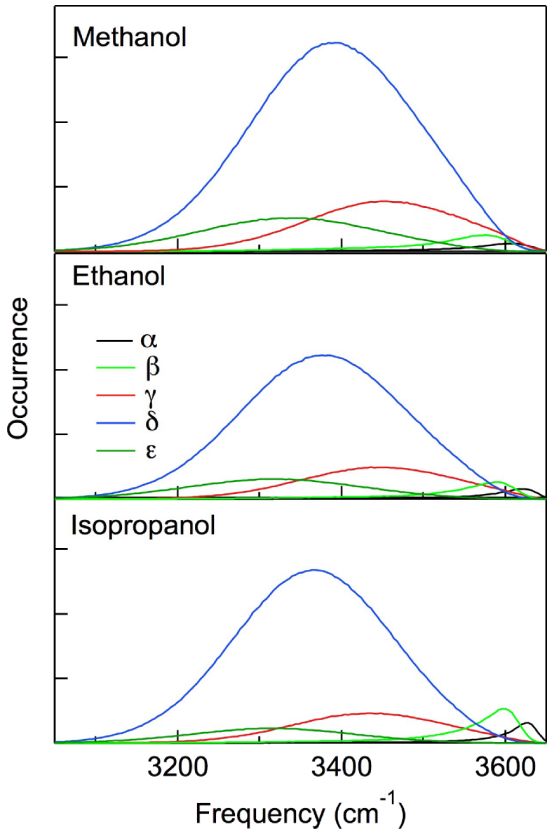

FIG. 4. Frequency histograms for the five different HB configurations presented for each of the three alcohols. The coloring scheme is identical to that of Fig. 3.

B. Pump-probe

Figure 5 shows the frequency-resolved pump-probe spectra of the three alcohols. Absorption decrease due to bleaching and stimulated emission (shown in blue) and increase due to induced absorption (shown in red) are observed at ~3350 cm^{-1} and ~3130 cm^{-1}, respectively. From the frequency difference between these two contributions, we estimate the anharmonic shift as ~220 cm^{-1}, which is close to the value used in the simulations. The development of the hot ground state due to vibrational thermalization is also apparent at times beyond 2 ps as evidenced by the red-shifted induced absorption.

To quantify the lifetime, we used a two-step relaxation model consisting of excited, intermediate, and hot ground states; the latter accounts for an increase of the temperature in the excited volume.[20,52] The initially excited OH stretching mode relaxes with the lifetime T_1 to the intermediate state, which in turn relaxes to the hot ground state with lifetime of T_{int}. The existence of the intermediate state is observed most directly in the experimental data by inspecting dynamics at the zero-crossing frequency, where bleaching and induced absorption compensate each other. Here, the signal increases with the time that is noticeably longer than the population time T_1. Therefore, it takes additional time T_{int} for the population to reach the hot ground state. Note the difference between definition of the intermediate state used here and that in Ref. 26: in the model[20,52] applied herein, the intermediate state is considered to be a dark state between the excited stretching mode and the hot ground state so that the excitation energy is transferred to low frequency modes indirectly. In contrast, in Ref. 26, the intermediate state is defined to mediate heat transfer from the alcohol cluster to the solvent bath which is absent in our study.

The population lifetime of the OH stretching mode deduced from this kinetic model (Figs. 5(b), 5(e), and 5(h)) amounts to ~630 fs, 720 fs, and 990 fs for methanol, ethanol, and isopropanol, respectively, with T_{int} = 350 ± 25 fs. Therefore, the lifetime becomes longer with the increase of the hydrophobic group. The OH stretch lifetime of ~700 fs in liquid water (HDO:D_2O) lies in between the three alcohols apparently indicating different relaxation pathways.[53] Unlike in the alcohol clusters,[18,20,54] artificial HB chains,[18,39,54] and deuterated bulk alcohols,[26] the lifetime does not seem to possess any distinct frequency dependence, at least in

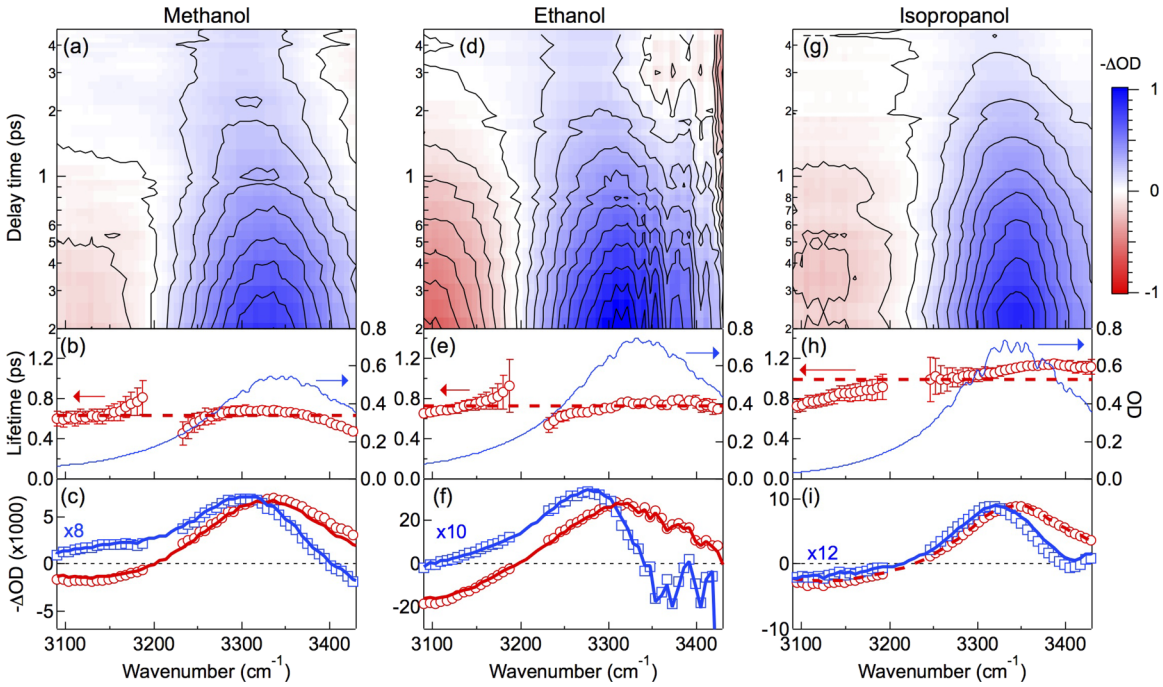

FIG. 5. Top panels: normalized frequency-resolved pump-probe signal; middle panels: frequency dependence of the OH stretch population lifetime (red) and linear absorption (blue); bottom panels: averaged in the range of 0.3-0.7 ps (red curve) and 4-20 ps (blue curve) transient absorption spectra, the scaled amplitudes of the fitting coefficients for the $|0\rangle - |1\rangle$ transition (red circles), and the hot ground state (blue squares) of methanol (left column), ethanol (middle column), and isopropanol (right column). Blue and red colors in (a), (d), and (g) correspond to absorption decrease and increase, respectively. The equidistant contours are drawn at each 10% of the maximal amplitude.

methanol and ethanol. This hints at efficient frequency mixing (spectral diffusion) at the time scale shorter than the population lifetime. Furthermore, the α- and β-type HB configurations that provide substantial contributions in the clusters and artificial chains are too scarce in bulk alcohols to contribute to the pump-probe signal. Nonetheless, a small frequency dependence of the lifetime in isopropanol seems to extend beyond the experimental uncertainty thereby suggesting the slower frequency mixing as compared to methanol and ethanol (see Sec. IV C).

VER pathways of the OH stretching mode in neat methanol have been extensively studied by IR/Raman spectroscopy.[24] It was concluded that different combinations of the OH bending mode, methyl rocking mode, CO stretching mode, and CH stretching modes of the same molecule act as energy acceptors. In the more recent study,[26] the OD relaxation time of bulk deuterated methanol in the methanol bath was measured as 0.75 fs, while for other alcohols (ethanol, 1-propanol, and 1-butanol) it amounted to 0.9 ps. The faster and frequency-dependent relaxation in methanol was explained by a Fermi resonance to the CH_3 rocking overtone at 2380–2440 cm^{-1}. In the case of the OH methanol oscillator, the relaxation as found here is even faster (0.63 ps) and cannot be explained by the Fermi resonance. This makes us conclude that collective effects play a prominent role in OH-stretch VER in bulk alcohols, similarly to water.[55,56]

C. 2D IR

Figure 6 presents experimental and calculated 2D IR spectra of the investigated alcohols at different waiting times. At short times, all spectra are diagonally elongated which indicates a frequency-correlated response of an inhomogeneously broadened system. With time, the memory for initial excitation frequency still persists, keeping the 2D signal slightly tilted. The calculated 2D spectra (lower panels in Fig. 6) present a reasonable agreement with the experiment.

To extract frequency correlations from the 2D spectrum, the center line slope (CLS) analysis[57] was applied in the frequency range of 3240–3415 cm^{-1} and 3225–3400 cm^{-1} in the calculations and experiment, respectively (Fig. 6, orange lines). In many cases, including non-Gaussian dynamics,[58,59] the CLS as a function of waiting time represents fairly well the frequency-frequency correlation function.

The results of the CLS analysis are summarized in Fig. 7. The time developments are similar for all three alcohols: the experimental CLS functions initially decay at a time scale of ~150 fs (140 fs, 110 fs, and 220 fs for methanol, ethanol, and isopropanol, respectively, with a 50% share) followed by a longer tail. In the simulations, the fast relaxation time is slower, ~500 fs (380 fs, 470 fs, and 660 fs for methanol, ethanol, and isopropanol, respectively), but the general trend of slowing down with the size of the alcohol molecule is well captured.

Faster correlation times in the experiment as compared to the simulations might arise from intermolecular Förster-like coupling between the OH oscillators.[28–31] However, in 6% methanol solution used in our experiments, the averaged distance between the non-deuterated molecules is ~1.1 nm which is much larger than the Förster radius of ~0.2 nm.[60] This is also consistent with the anisotropy data in Ref. 26 where the substantial anisotropy drop began at ~10% concentration and our anisotropy data where the initial anisotropy value is close

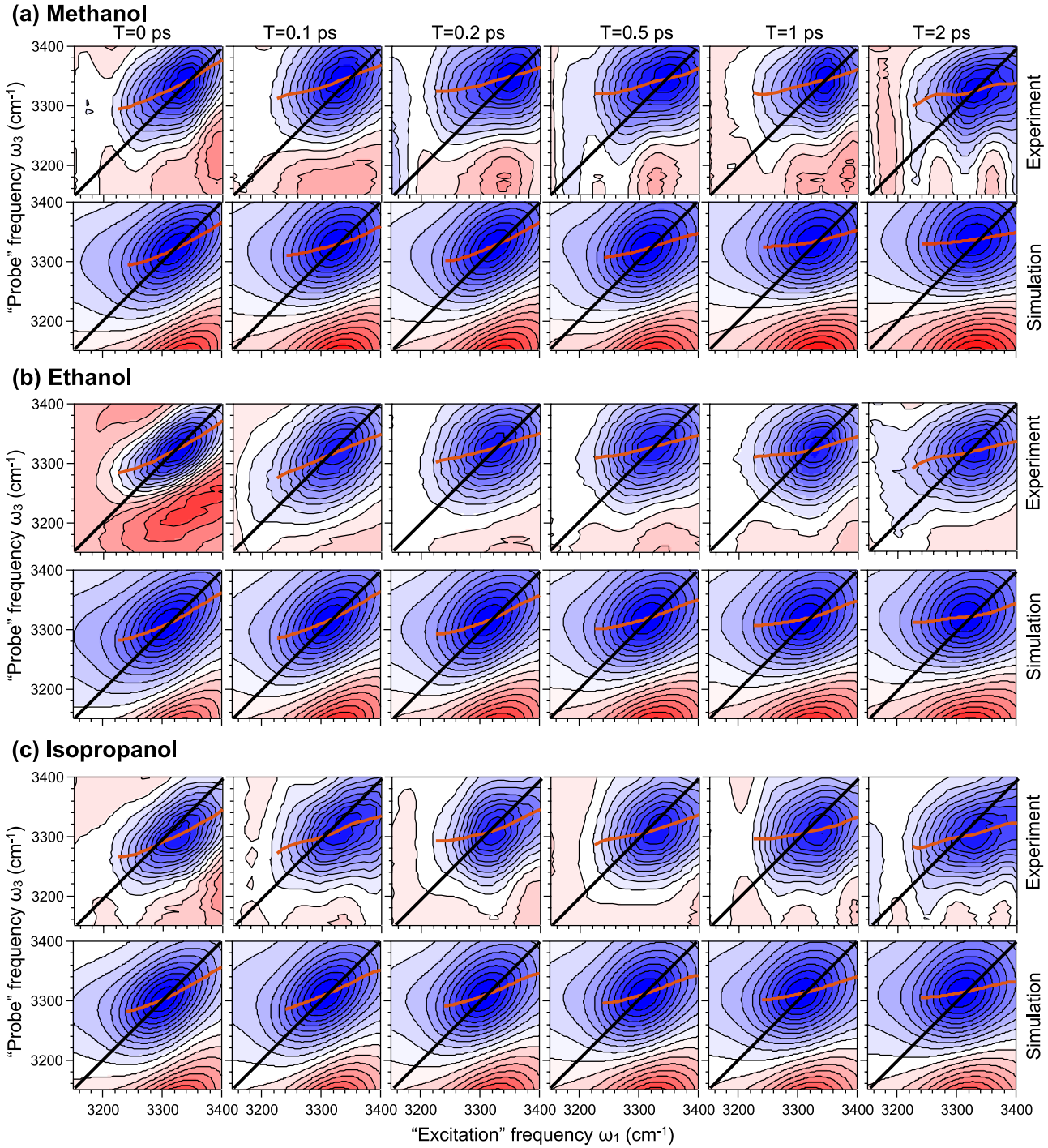

FIG. 6. Normalized experimental (top panels) and simulated (bottom panels) absorptive 2D spectra of (a) methanol, (b) ethanol, and (c) isopropanol at different waiting times. Blue and red colors correspond to absorption decrease and increase, respectively. Thick orange lines show the results of the CLS analysis. The equidistant contours are drawn at each 10% of the maximal amplitude.

to 0.4 (see Sec. IV D). Therefore, the Förster energy transfer does not contribute to the experimental CLS values.

According to the MD simulations, the fast component originates from fluctuations within a given HB configuration as librations and the HB stretching mode which is supported by the broad frequency distributions in Figure 4. These molecular motions provide fast and efficient spectral diffusion to make the OH population lifetime independent of frequency (see Fig. 5). The simulations overestimate these time scales, most probably due to a combination of inaccuracies in the hydrogen bond dynamics predicted by the used force fields, large sensitivity to sampling noise,[62] and the presence of non-Gaussian dynamics leading to slightly curved slope lines at short times.[58,59] In any case, the fast time scales are slower than that for HDO:D_2O and HDO:H_2O (~50 fs).[29,30] The slow relaxation constants obtained from the simulations are 4 ps, 7 ps, and 14 ps, again in a sharp contrast to the HDO:D_2O case, where no such long tail is observed.

To understand the CLS relaxation times, the HB dynamics was analyzed by determining the time during which each

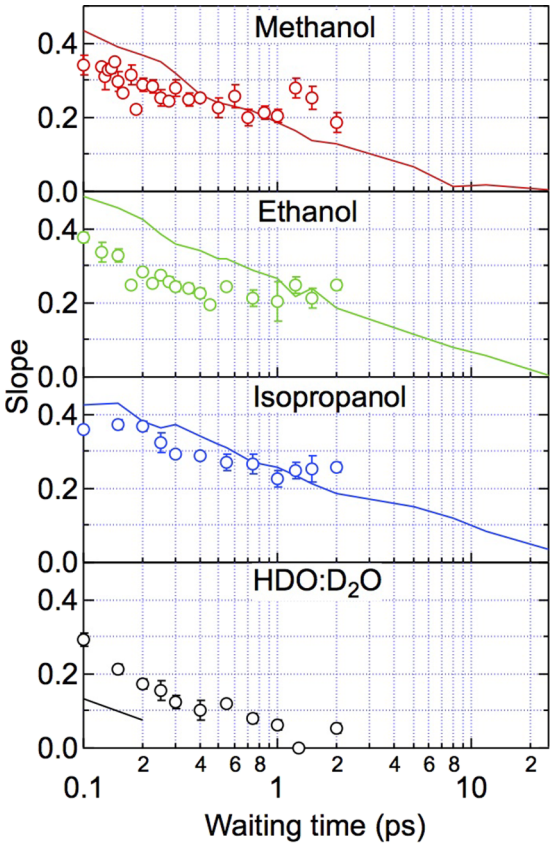

FIG. 7. The experimental (open circles) and simulated (solid lines) CLS values for methanol (a), ethanol (b), isopropanol (c), and HDO:D_2O ((d), solid line is taken from Ref. 61) as functions of the waiting time.

alcohol molecule donor is bound to the same acceptor. These times were determined for all alcohol molecules in the full MD trajectories and counted in the histograms displayed in Fig. 8. Here, the number of exchanges with a given lifetime is shown and normalized by the bin width, the number of alcohol molecules in the simulation box, and the trajectory length (500 ps). Therefore, the units on the y-axis are the number of exchanges per alcohol molecule per ps. The HB lifetime distributions were fitted using a triexponential function for

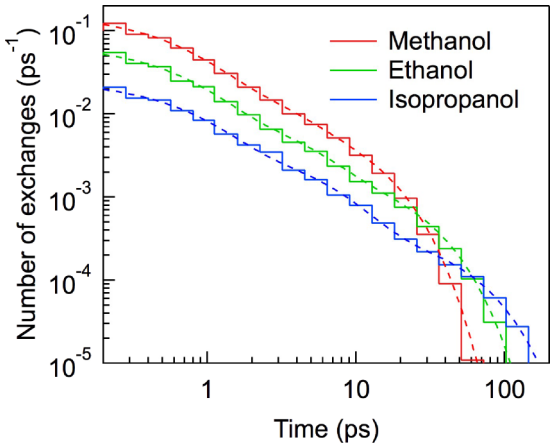

FIG. 8. Histograms of the number of HB exchange events with a given lifetime per molecule per ps (solid lines). The dashed lines are triexponential fits using a weighted error function proportional to the amplitude to capture both long and short times. The fit parameters are given in Table I.

TABLE I. The parameters obtained from the triexponential fits of the HB lifetime histograms in Fig. 8. All times are given in ps, while the unit of the coefficients A_i is ps^{-1}.

	A_1 (ps^{-1})	T_1 (ps)	A_2 (ps^{-1})	T_2 (ps)	A_3 (ps^{-1})	T_3 (ps)
Methanol	0.128	0.53	0.023	2.1	0.010	9.5
Ethanol	0.058	0.57	0.010	3.2	0.0022	20.3
Isopropanol	0.021	0.66	0.004	4.9	0.0004	45.2

which the fitting parameters are presented in Table I. Overall, methanol exhibits most HB exchanges, which explains differences in the fastest time scale. However, after about 20 ps, fewer exchanges occur in methanol than in the other two alcohols. In particular, isopropanol has more HB configurations lasting longer than 60 ps than the smaller alcohols have. This directly influences tails of the CLS functions as each HB exchange disrupts the frequency correlation function. The hydrogen bond exchange times found there are somewhat different from those reported in Ref. 63. This may be due to the use of different hydrogen bond criteria. Furthermore, the united atom force field used in Ref. 63 may result in lower viscosities.

The effect of HB exchange on the frequency correlation function can be understood from the analysis of the change of the frequency around the time of a HB exchange. For this, we define the time of the HB exchange as the time where the OH stretch frequency of the donor is the highest in the vicinity of time around a change of acceptor partner. In spirit similar to the HB jump analysis by Laage *et al.*,[4,64,65] here we, however, directly used the spectroscopically observable OH-frequency to set the time of the exchange event instead of using a geometric HB criterion.

In Fig. 9, the time-evolution of the average frequency of the donor and the two involved acceptors are presented along with the time evolution of the average angular velocity of the OH bonds. We found very similar behavior for the three different alcohols. The involved donor may be a γ, δ, or ε configuration; however, from the average frequency, it can be seen that the higher frequency γ configurations are more likely donors. Only β, δ, and ε may be initial acceptors, while the final acceptors are of the α, β, γ, or δ-type. The donor is intermittently losing the donated HB giving rise to a sharp increase in the OH-stretch frequency of the donor molecules.

Following the exchange, the donor returns to the same type of configuration that it has come from. The initial acceptor has lost a HB, and the frequency of its OH-stretch vibration has, thus, slightly increased, while the final acceptor gaining a HB has received a slightly lower OH-stretch frequency. Overall, the effect of the HB exchange on the frequency is rather small. Furthermore, due to the non-Condon effect,[48] the intermittent transition of the donor through an α or β configuration hardly affects the slopes in the two-dimensional spectra as the transition dipole of these states is very low. In contrast, the frequency correlation functions that are not dependent on the transition dipole are strongly affected by the presence of the transition state. Therefore, the observed CLS functions mainly reflect the fluctuations within the dominating δ configurations and to a much smaller extend the HB exchange induced by

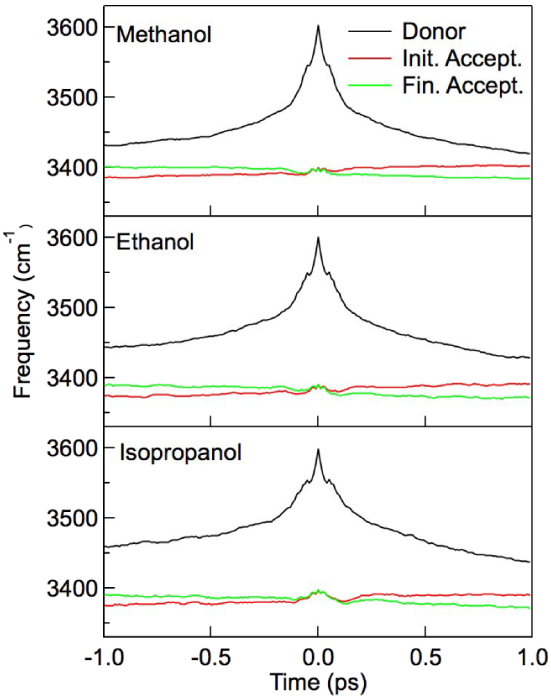

FIG. 9. The time evolution of the average frequencies of the OH stretching mode around the time of a HB exchange event.

transformations of HB acceptors between the γ, δ, and ε configurations, which differ considerably in average frequency according to the frequency distributions given in Figure 4.

The amount of frequency correlation persisting through a HB exchange event was investigated by calculating the correlation of the OH stretch frequency 1 ps before the exchange and 1 ps after the exchange using the following equation, which essentially a normalized frequency auto-correlation function synchronized to be centered at the time of the HB exchanges:

$$C(t) = \frac{\langle \omega(t-1ps)\cdot\omega(t+1ps)\rangle}{\sqrt{\langle \omega(t-1ps)\cdot\omega(t-1ps)\rangle\cdot\langle \omega(t+1ps)\cdot\omega(t+1ps)\rangle}}. \quad (3)$$

Here, t is the time of a HB exchange event and the brackets denote an average over all HB exchanges. For the donor molecules, the correlation preserved through a HB exchange event amounts to 9%, 18%, and 23% for methanol, ethanol, and isopropanol, respectively. Somewhat surprisingly, the correlation preserved through a HB exchange event for the acceptor alcohols is a bit lower, with 7%, 10%, and 20% values for the three alcohols. This is explained in the light that the HB exchange event does alter the HB configuration of the acceptor resulting in considerable frequency changes according to Figure 4, while the donor returns to its original HB type following a HB event.

The delay time of 1 ps in Eq. (3) is somewhat arbitrary, but at all shorter times, the same tendency of lower memory loss for the donors is observed. For instance, for 40 fs time instead of 1 ps, the values for donors are 75%, 78%, and 81%, while the numbers for acceptors are 64%, 67%, and 73% for the three alcohols, respectively. Therefore, the difference between donors and acceptors is preserved for very long times.

D. Anisotropy

Whereas HB strength fluctuations of the dominant δ configurations were determined from the waiting time dependence of the 2D IR line shapes, the angular motion is studied through the polarization anisotropy. Figure 10 shows rotational anisotropy of the investigated alcohols, determined at the maximum bleach position. The theoretical anisotropy was derived from the calculated parallel- and perpendicularly polarized 2D spectra using Eq. (1); it excellently corroborates experimental data. At the beginning, the anisotropy is close to its limiting value of 0.4 which indicates that intermolecular coupling between the OH oscillators is low because of dilution. At later times, the anisotropy relaxes with times that become longer with the hydrophobic group length. These features are well reproduced by the calculation even despite the limited experimental delay range due to OH stretch depopulation. Anisotropy for all alcohols decays noticeably slower than for water[66] (Fig. 10(d)). The anisotropy decay rate is also independent of the probe frequency between 3250 and 3400 cm^{-1} in sharp contrast to HDO:H$_2$O,[67] where faster dynamics in the high-frequency wing were assigned to HB breaking, while the slower dynamics in the low-frequency wing were attributed to HB reformation.

Time constants of anisotropy dynamics are calculated by fitting the simulation curves with a bi-exponential function. This results in fast time constants of 200 fs, 340 fs, and 370 fs (contribution of ~15%) and slow time constants of 4.6 ps,

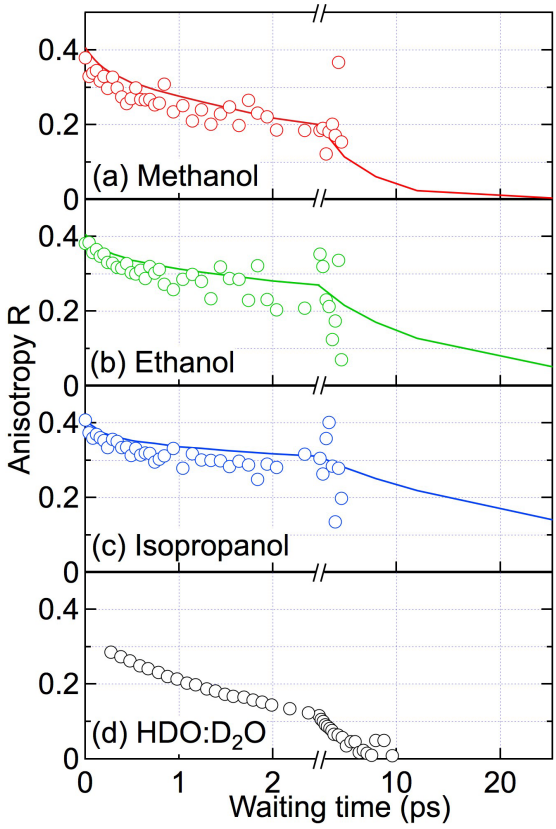

FIG. 10. The experimental (open circles) and simulated (solid lines) transient rotational anisotropy probed at 3300 cm^{-1} of methanol (red), ethanol (green), isopropanol (blue), and water (black, Reproduced by permission from Rezus and Bakker, J. Chem. Phys. **123**, 114502 (2005) for comparison).

12 ps, and 27 ps for methanol, ethanol, and isopropanol, respectively. The slow time scales are in reasonable agreement with the nuclear magnetic resonance (NMR) data of 5 ps,[68] 12-18 ps,[68–70] and 33 ps[68] for the three alcohols, respectively, although calculated values for ethanol and isopropanol appear 20%-25% faster. It is also worth noticing that we do not confirm the 1-4 ps time scales reported in Ref. 26 and assigned to reorientation of molecules with intact HBs. In turn, Mazur *et al.*[26] did not observe the sub-ps time scales seen by us and others.[71]

Debye relaxation studies[72] reported much longer time scales of 51, 163, and 329 ps for methanol, ethanol, and isopropanol, respectively. However, Debye relaxation depends on the first-order rotational correlation function of the dipole of the solution, while the anisotropy decay depends on the second-order dipole correlation function of the OH-stretch transition dipole. While a rule of thumb[73] suggests that the time scales related to the Debye relaxation are by a factor of 3 slower than the anisotropy decay and experiments on water have suggested a factor of 3.4 difference,[74] one should be cautious by comparing these numbers directly as they relate the reorientation of different vectors. Furthermore, Debye response is also affected by dipole-induced dipole interactions due to polarizability of the alcohol molecules.[75] In particular, it was reported that the slow component of the Debye relaxation is due to collective effects.[75]

To explain the observed time scales, we calculated the average angular velocity of the OH groups during the HB exchange (Fig. 11). On average, the overall angular velocity of the OH bonds is about 0.7°/fs, which corresponds to the thermal energy of the librational motion of a hydrogen atom. For the donor alcohol, the angular velocity starts increasing about 0.5 ps before the actual HB exchange and peaks just before and again just after the moment, where the OH-stretch frequency peaks. The dip at time zero reflects the pass through the transition state, where the kinetic energy has been converted to potential energy. The very short duration of the actual exchange event (~40 fs) corresponds to one period of the librational motion (frequency of ~800 cm^{-1}) of the donor hydrogen that dominates the reaction coordinate. This agrees very well to the findings previously reported for the hydrogen jump mechanism of water[4] and alcohols.[63] Upon very close inspection, it is seen that the angular velocity of the initial acceptor is increasing at the time of the exchange and the angular velocity of the final acceptor decreases. This can be understood as a reflection of the fact that the stronger hydrogen bonded ε configuration exhibits slightly slower rotational dynamics than the weakly bound γ configuration. However, the acceptors are unlikely to contribute to an anisotropy change due to exchange events thereby leaving dominating contribution to the donors.

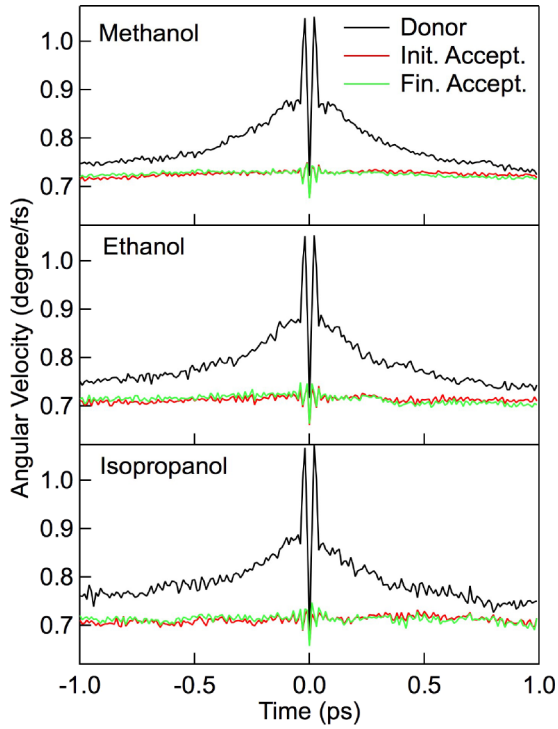

FIG. 11. The time evolution of the average angular velocity of the OH bonds around the time of a HB exchange event.

Therefore, there are two main processes that contribute to the anisotropy decay. The fastest time scales are related to wobbling-in-a-cone type dynamics, which are essentially similar for the three alcohols. The slow time scales are related to HB exchange dynamics in accordance with the orientational jump model developed for water[76] and frame reorientation with intact HB as reported for bulk methanol and ethanol.[63] The different time constants between the three alcohols are explained by the slower diffusional motion, required to trigger the orientational jump, of the molecules with longer alkyl chains.[77] The frame reorientation is naturally connected with the diffusion in a similar way as the slow orientational jumps,[63] and this contribution is expected to behave identically to the slow exchange dynamics. This makes it difficult to determine the actual relative importance of the two for the slow anisotropy decay.

E. Discussion

The dynamics in alcohols can briefly be summarized as follows. On the sub-picosecond time scale, dynamics is governed by librational motion of the wobbling-in-a-cone type and HB stretch motion dominated by the contribution from the most abundant δ-type HB configuration. The slower motion is found in all alcohols reflecting the HB exchange dynamics. However, the exact mapping of these dynamics depends on a particular experimental arrangement. The 2D IR spectroscopy is dominated by the frequency change experienced by the involved *acceptors*. In contrast, the anisotropy transients are dominated by reorientation of the *donors*.

To find a correlation between the slowest time scales of the observed properties and the diffusion motion, we calculated the diffusional constants as 2.57, 1.29, and $0.63 \cdot 10^{-5}$ cm^2/s for methanol, ethanol, and isopropanol, respectively. Experimentally, the diffusion constant for methanol was reported to be $2.37 \cdot 10^{-5}$ cm^2/s,[78] in good agreement with our theoretical findings. Figure 12 shows the relation between the inverse diffusion constant (D) for the three alcohols and the slowest calculated time scales in the anisotropy decay, the CLS, and the HB exchange dynamics is approximately linear. The slow time scales are all different due to the differences in the magnitude of

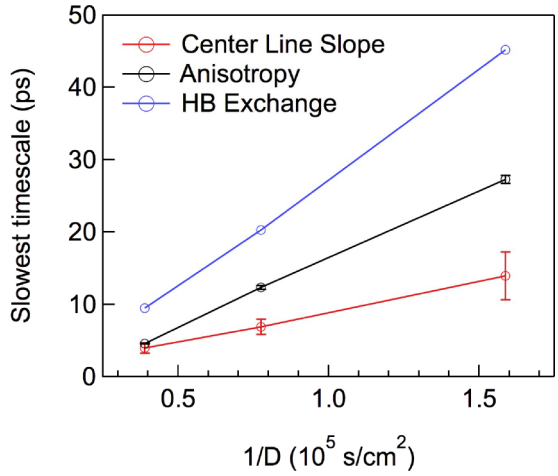

FIG. 12. The relation between the slowest calculated time scales of the anisotropy decay, the CLS, and the HB exchange dynamics and the inverse diffusion constant D for the three alcohols.

frequency and angular changes upon HB exchange. Therefore, this analysis suggests a universal relation between the slow time scales and the diffusional motion, which reflects that all these slow dynamics are dictated by the HB exchange.

Here, we have found a linear correlation between the slow components of the studied dynamics with the diffusion constant, but not demonstrated the mechanism behind this proposed universal scaling behavior. It is possible that the reason that both the slow parts of the CLS, anisotropy, and HB exchange scale inversely with the diffusion constant is that these processes share a common underlying physical mechanism with diffusion. This could be the activated transition between hydroxyls in the first and second transition shell of a given hydroxyl. The presented relationship is further related to the Stokes-Einstein-Debye relation suggesting the relation between translational and rotational diffusions for spherical particles: $D = k_BT/6\pi\eta R_H = 4R_H^2D_{rot}$, where η is the viscosity, R_H is the hydrodynamic radius, and D_{rot} is the rotational diffusion constant.[79,80] The latter is sometimes assumed to be inversely proportional to the dielectric relaxation times,[81] thus suggesting an inverse relationship between the dielectric relaxation time and the translational diffusion times. We further note that in Ref. 63, the difference between the behaviour of methanol, ethanol, and water was attributed to an excluded-volume effect. This may very well be related to our findings as one would expect that diffusion is needed to overcome the excluded-volume effect. Future systematic experimental studies determining both the diffusion constant and the dynamical properties under comparable conditions for a larger number of alcohols than we could examine here should be able to validate and find the possible limits of the proposed universal scaling.

Finally, the difference of HB structure and dynamics between water and alcohols can be discussed. In liquid water, most molecules have three or four HBs, which results in a heterogeneous three-dimensional HB network. In alcohols, the δ-type HB configuration dominates resulting in a more homogeneous distribution of chain and/or ring-like HB structures. This explains the narrowing of the linear absorption in alcohols as compared to water. In water, there is a high density of HB acceptors and donors, while in the alcohols, the density is lower (in particular, of available donors). This leads to the emergence of slow diffusion controlled HB exchange dynamics in alcohols, which is essentially absent in water. These slow dynamics are responsible for the long tails observed in the experimental anisotropy decay and CLS. On the other hand, the fast sub-ps dynamics in water and alcohols is rather comparable with each other, as it is dominated by the similar librational and HB stretch motion.

V. CONCLUSIONS

We have investigated the HB dynamics in three liquid alcohols by 2D IR spectroscopy and MD simulations combined with quantum-classical spectral simulations. During the experimentally accessible time scales, the experiments and theory exhibit good agreement allowing us to use the MD simulation for understanding the HB dynamics well beyond the OH stretch vibrational lifetime. The HB dynamics occur on two prime time scales. The fastest of these reflects phase memory loss attributed to librational and translational HB fluctuations. Interestingly, the fast component of the dynamics appears to be essentially universal to hydrogen bonded systems including previously studied water and alcohol chains. The longer time scales are manifestations of the HB exchange that are unique for the bulk alcohols. The HB exchange dynamics observed in diluted alcohols have little or no relevance for the bulk.

Although different spectroscopic observables provide disparate relaxation times, the simulations suggest that they are all correlated with the inverse of the diffusion constant reflecting an intricate relation between the HB dynamics and the diffusional motion. The larger alcohols having smaller diffusion constants thus exhibit slower HB exchange dynamics, anisotropy decay, and spectral diffusion. While only three different alcohols are investigated here, a universal scaling behavior relating HB exchange and diffusion is proposed. This may be based on a common underlying mechanism as the activated transfer of molecules between different solvation shells. Such fundamental scaling relationship will likely impact the understanding of processes in chemistry and biology, where hydrogen bonding plays a crucial role.

ACKNOWLEDGMENTS

D. A. Wiersma is gratefully acknowledged for his enthusiastic support of this project.

[1]M. Fayer, *Ultrafast Infrared Vibrational Spectroscopy* (CRC Press, 2013).
[2]P. Hamm and M. Zanni, *Concepts and Methods of 2D Infrared Spectroscopy* (Cambridge University Press, 2011).
[3]M. Cho, *Two-Dimensional Optical Spectroscopy* (CRC Press, 2009).
[4]D. Laage and J. T. Hynes, Science **311**, 832 (2006).
[5]A. Tokmakoff, Science **317**, 54 (2007).
[6]M. L. Cowan, B. D. Bruner, N. Huse, J. R. Dwyer, B. Chugh, E. T. J. Nibbering, T. Elsaesser, and R. J. D. Miller, Nature **434**, 199 (2005).
[7]S. T. Roberts, K. Ramasesha, and A. Tokmakoff, Acc. Chem. Res. **42**, 1239 (2009).
[8]Y. Umena, K. Kawakami, J.-R. Shen, and N. Kamiya, Nature **473**, 55 (2012).
[9]T. Sun, Science **343**, 795 (2014).
[10]S. K. Pal, J. Peon, and A. H. Zewail, Proc. Natl. Acad. Sci. U. S. A. **99**, 1763 (2002).
[11]M. Chaplin, Nat. Rev. Mol. Cell Biol. **7**, 861 (2006).

[12]J. Israelachvili and H. Wennerström, Nature **379**, 219 (1996).
[13]A. A. Bakulin, M. S. Pshenichnikov, H. J. Bakker, and C. Petersen, J. Phys. Chem. A **115**, 1821 (2011).
[14]D. Laage, G. Stirnemann, and J. T. Hynes, J. Phys. Chem. B **113**, 2428 (2009).
[15]Y. Rezus and H. Bakker, Phys. Rev. Lett. **99**, 148301 (2007).
[16]R. Laenen, G. M. Gale, and N. Lascoux, J. Phys. Chem. A **103**, 10708 (1999).
[17]S. Woutersen, U. Emmerichs, and H. J. Bakker, J. Chem. Phys. **107**, 1483 (1997).
[18]K. J. Gaffney, P. H. Davis, I. R. Piletic, N. E. Levinger, and M. D. Fayer, J. Phys. Chem. A **106**, 12012 (2002).
[19]R. Laenen and C. Rauscher, J. Phys. Chem. A **101**, 3201 (1997).
[20]J. B. Asbury, T. Steinel, C. Stromberg, K. J. Gaffney, I. R. Piletic, and M. D. Fayer, J. Chem. Phys. **119**, 12981 (2003).
[21]R. Laenen and K. Simeonidis, Chem. Phys. Lett. **299**, 589 (1999).
[22]R. Laenen and C. Rauscher, Chem. Phys. Lett. **274**, 63 (1997).
[23]E. J. Heilweil, M. P. Casassa, and R. R. Cavanagh, J. Chem. Phys. **85**, 5004 (1986).
[24]L. K. Iwaki and D. D. Dlott, J. Phys. Chem. A **104**, 9101 (2000).
[25]K. Kwac and E. Geva, J. Phys. Chem. B **117**, 7737 (2013).
[26]K. Mazur, M. Bonn, and J. Hunger, J. Phys. Chem. B **119**, 1558 (2015).
[27]J. Helbing and P. Hamm, J. Opt. Soc. Am. B **28**, 171 (2011).
[28]S. Woutersen, U. Emmerichs, and H. J. Bakker, Science **278**, 658 (1997).
[29]J. B. Asbury, T. Steinel, K. Kwak, S. A. Corcelli, C. P. Lawrence, J. L. Skinner, and M. D. Fayer, J. Chem. Phys. **121**, 12431 (2004).
[30]C. J. Fecko, J. D. Eaves, J. J. Loparo, and A. Tokmakoff, Science **301**, 1698 (2003).
[31]S. Yeremenko, M. S. Pshenichnikov, and D. A. Wiersma, Chem. Phys. Lett. **369**, 107 (2003).
[32]H. Berendsen and D. van der Spoel, Comput. Phys. Commun. **91**, 43 (1995).
[33]W. L. Jorgensen, A. D. S. Maxwell, and J. Tirado-Rives, J. Am. Chem. Soc. **118**, 11225 (1996).
[34]U. Essmann, L. Perera, M. L. Berkowitz, T. Darden, H. Lee, and L. G. Pedersen, J. Chem. Phys. **103**, 8577 (1995).
[35]H. J. C. Berendsen, J. P. M. Postma, W. F. van Gunsteren, A. DiNola, and J. R. Haak, J. Chem. Phys. **81**, 3684 (1984).
[36]B. Hess, H. Bekker, H. J. C. Berendsen, and J. G. E. M. Fraaije, J. Comput. Chem. **18**, 1463 (1997).
[37]W. Humphrey, A. Dalke, and K. Schulten, J. Mol. Graphics **14**, 33 (1996).
[38]B. Auer, R. Kumar, J. R. Schmidt, and J. L. Skinner, Proc. Natl. Acad. Sci. U. S. A. **104**, 14215 (2007).
[39]C. P. van der Vegte, S. Knop, P. Vöhringer, J. Knoester, and T. L. C. Jansen, J. Phys. Chem. B **118**, 6256 (2014).
[40]C. P. van der Vegte, A. G. Dijkstra, J. Knoester, and T. L. C. Jansen, J. Phys. Chem. A **117**, 5970 (2013).
[41]F. Li and J. L. Skinner, J. Chem. Phys. **132**, 204505 (2010).
[42]T. L. C. Jansen, T. Hayashi, W. Zhuang, and S. Mukamel, J. Chem. Phys. **123**, 114504 (2005).
[43]C. Liang and T. L. C. Jansen, J. Chem. Theory Comput. **8**, 1706 (2012).
[44]K. Kwac and E. Geva, J. Phys. Chem. B **115**, 9184 (2011).
[45]O. Kristiansson, J. Mol. Struct. **477**, 105 (1999).
[46]S. S. Farwaneh, J. Yarwood, and I. Cabaço, J. Mol. Liq. **56**, 317 (1993).
[47]R. Kumar, J. R. Schmidt, and J. L. Skinner, J. Chem. Phys. **126**, 204107 (2007).
[48]J. R. Schmidt, S. A. Corcelli, and J. L. Skinner, J. Chem. Phys. **123**, 044513 (2005).
[49]C. P. Lawrence and J. L. Skinner, J. Chem. Phys. **117**, 8847 (2002).
[50]T. Steinel, J. B. Asbury, S. A. Corcelli, and C. P. Lawrence, Chem. Phys. Lett. **386**, 295 (2004).
[51]K. B. Møller, R. Rey, and J. T. Hynes, J. Phys. Chem. A **108**, 1275 (2004).
[52]S. Yeremenko, M. Pshenichnikov, and D. Wiersma, Phys. Rev. A **73**, 021804 (2006).
[53]J. J. Loparo, C. J. Fecko, J. D. Eaves, and S. T. Roberts, Phys. Rev. B **70**, 180201(R) (2004).
[54]S. Knop, T. La Cour Jansen, J. Lindner, and P. Vöhringer, Phys. Chem. Chem. Phys. **13**, 4641 (2011).
[55]J. Lindner, P. Vöhringer, and M. S. Pshenichnikov, Chem. Phys. Lett. **421**, 329 (2006).
[56]J. Lindner, D. Cringus, M. S. Pshenichnikov, and P. Vöhringer, Chem. Phys. **341**, 326 (2007).
[57]K. Lazonder, M. S. Pshenichnikov, and D. A. Wiersma, Opt. Lett. **31**, 3354 (2006).
[58]S. Roy, M. S. Pshenichnikov, and T. L. C. Jansen, J. Phys. Chem. B **115**, 5431 (2011).
[59]T. L. C. Jansen, D. Cringus, and M. S. Pshenichnikov, J. Phys. Chem. A **113**, 6260 (2009).
[60]K. J. Gaffney, I. R. Piletic, and M. D. Fayer, J. Chem. Phys. **118**, 2270 (2003).
[61]T. L. C. Jansen, B. M. Auer, M. Yang, and J. L. Skinner, J. Chem. Phys. **132**, 224503 (2010).
[62]J. F. Kruiger, C. P. van der Vegte, and T. L. C. Jansen, J. Chem. Phys. **142**, 054201 (2015).
[63]A. A. Vartia, K. R. Mitchell-Koch, G. Stirnemann, D. Laage, and W. H. Thompson, J. Phys. Chem. B **115**, 12173 (2011).
[64]D. Laage, G. Stirnemann, F. Sterpone, and J. T. Hynes, Acc. Chem. Res. **45**, 53 (2012).
[65]D. Laage, G. Stirnemann, and J. T. Hynes, J. Photochem. Photobiol., A **234**, 75 (2012).
[66]Y. L. A. Rezus and H. J. Bakker, J. Chem. Phys. **123**, 114502 (2005).
[67]S. T. van der Post and H. J. Bakker, J. Phys. Chem. B **118**, 8179 (2014).
[68]R. Ludwig, M. D. Zeidler, and T. C. Farrar, Z. Phys. Chem. **189**, 19 (1995).
[69]R. Ludwig and M. D. Zeidler, Mol. Phys. **82**, 313 (1994).
[70]T. D. Ferris and T. C. Farrar, Mol. Phys. **100**, 303 (2002).
[71]R. Buchner and J. Barthel, J. Mol. Liq. **52**, 131 (1992).
[72]J. Barthel, K. Bachhuber, R. Buchner, and J. B. Gill, Chem. Phys. Lett. **167**, 62 (1990).
[73]J. Hunger, A. Stoppa, A. Thoman, M. Walther, and R. Buchner, Chem. Phys. Lett. **471**, 85 (2009).
[74]K. J. Tielrooij, C. Petersen, Y. L. A. Rezus, and H. J. Bakker, Chem. Phys. Lett. **471**, 71 (2009).
[75]B. M. Ladanyi and M. S. Skaf, J. Phys. Chem. **100**, 1368 (1996).
[76]R. Jiang and E. L. Sibert III, J. Phys. Chem. A **113**, 7275 (2009).
[77]A. A. Bakulin, D. Cringus, P. A. Pieniazek, J. L. Skinner, T. L. C. Jansen, and M. S. Pshenichnikov, J. Phys. Chem. B **117**, 15545 (2013).
[78]L. A. Woolf, Pure Appl. Chem. **57**, 1083 (1985).
[79]A. Einstein, Ann. Phys. **324**, 371 (1906).
[80]I. Chang and H. Sillescu, J. Phys. Chem. B **101**, 8794 (1997).
[81]C. Lederle, W. Hiller, C. Gainaru, and R. Böhmer, J. Chem. Phys. **134**, 064512 (2011).